Plasmonics (2013) 8:283–287
DOI 10.1007/s11468-012-9387-8

Design of Optical Filters with Flat-on-Top Transmission Lineshapes Based on Two Side-Coupled Metallic Grooves

Xu-Sheng Lin · Sheng Lan

Received: 20 March 2012 / Accepted: 27 May 2012 / Published online: 6 June 2012

Abstract We investigate theoretically and numerically the resonant transmission through side-coupled metallic grooves. In the framework of coupled mode theory (CMT), a single metallic groove can be considered as a lossy optical resonator and two metallic grooves coupled via tunneling effect can be treated as a second-order cascade resonator. The relationship between the transmission lineshape of the coupled grooves and the cross-coupling between the grooves is analyzed by CMT. It is found that a flat-on-top lineshape can be obtained when the cross-coupling is equal to the total decay rate of the groove mode. Predictions based on the CMT analysis are in good agreement with the simulation results based on the finite-difference time-domain technique.

Keywords Surface plasmon polariton · Metallic groove · Tunneling

Abbreviations

SPPs	surface plasmon polaritons
CMT	coupled mode theory
FDTD	finite-difference time-domain method

X.-S. Lin · S. Lan (✉)
Laboratory of Nanophotonic Functional Materials and Devices, School of Information and Optoelectronic Science and Engineering, South China Normal University, Guangzhou 510006, China
e-mail: slan@scnu.edu.cn

X.-S. Lin
School of Electronic and Information Engineering, Guangdong Polytechnic Normal University, Guangzhou 510665, China

Introduction

Subwavelength metallic grooves play an important role in the study of surface plasmon polaritons (SPPs). For instance, they have been used to excite SPPs in groove–slit structures [1, 2], to realize unidirectional SPP propagation along metal surface [3], to guide channel SPPs in a low-loss and well-confined manner [4], etc. Besides, metallic grooves have been employed in many SPP-assisted processes, such as the enhancement of light absorption in solar cells and the optical elements of switching and filtering where strong localization of wave energy is required [5–7]. Actually, the strongly localized energy comes from the localized SPP modes formed by multireflection or scattering of the guiding SPPs in grooves. It has been well known that the resonant tunneling of these localized modes can lead to large transmission through metal gratings [8–12]. People consider it as the major mechanism of extraordinary transmission through metallic films with an array of holes, in the sense that a subwavelength hole can only support evanescent waves [8, 9, 13]. Therefore, the study of the resonant tunneling of localized SPP modes is very important from the viewpoints of both fundamental research and device application. Obviously, the investigation of the tunneling between two grooves rather than two gratings is of more fundamental. To the best of our knowledge, however, this issue remains unresolved. In this article, we introduce a parameter (cross coupling) to characterize the tunneling effect between two metallic grooves and derive the formula for the transmission. Since a single groove can be considered as a lossy optical resonator, two metallic grooves coupled via tunneling effect can be treated as a second-order cascade resonator. Thus, the transmission behavior of coupled grooves can be analyzed by using coupled mode theory (CMT) [14]. With the advance and development of plasmonic

devices, SPP tunneling is found to be an important physical mechanism for optical filters based on subwavelength metallic structures. Similar to traditional optical filters, optical filters relying on SPP tunneling with flat tops and sharp edges are highly desirable especially in the system of wavelength division multiplexing because the cross-talk between adjacent channels can be significantly reduced while the optical signal can be effectively transferred with negligible distortion. Such characteristics can be achieved by modifying the cross-coupling of coupled metallic grooves. We compare the CMT predictions with the simulation results based on the finite-difference time-domain (FDTD) technique and find a good agreement between them. Therefore, the investigation of metallic grooves based on CMT analysis and FDTD simulation would be helpful for the design of optical filters relying on SPP tunneling.

An Isolated Metallic Groove

Before discussing coupled groove structures, it is necessary to understand the resonant modes of an isolated groove. The physical model for the isolated groove is schematically shown in Fig. 1. A thin silver layer (represented by orange color) with a U-shaped groove is embedded in silica (represented by green color). The width of the groove is designed to be much smaller than the wavelength of the incident wave so that only the fundamental mode can be excited in it. When an electromagnetic wave with transverse magnetic polarization is launched normally on the groove from the left side, it will be reflected at both the mouth and the bottom of the groove. Thus, the groove acts as a Fabry–Pérot resonator.

Suppose a is the amplitude of the localized groove mode whose resonant frequency is ω_0, γ_{ref} is the decay rate of a into the reflected wave, γ_0 is the total decay rate of a into other channels that include scattering, excitation of SPPs, and absorption, i.e., $\gamma_0 = \gamma_{sca} + \gamma_{SPP} + \gamma_{ab}$, then the following relationship can be established based on CMT

$$\begin{cases} \frac{da}{dt} = (j\omega_0 - \gamma_{ref} - \gamma_0)a + \sqrt{2\gamma_{ref}}s_{in} \\ s_{ref} = -s_{in} + \sqrt{2\gamma_{ref}}a \end{cases}, \quad (1)$$

where s_{in} and s_{ref} are the normalized amplitudes of the incident and reflected waves, respectively. Thus, $|s_{in}|^2$ and $|s_{ref}|^2$ represent the incident and reflected powers. Consequently, the reflectance, defined as $R=|s_{ref}/s_{in}|^2$, and the localized energy in the groove, expressed as $|a|^2$, can be derived as

$$\begin{cases} R = \frac{(\omega-\omega_0)^2+(\gamma_{ref}-\gamma_0)^2}{(\omega-\omega_0)^2+(\gamma_{ref}+\gamma_0)^2} \\ |a|^2 = \frac{2\gamma_{ref}}{(\omega-\omega_0)^2+(\gamma_0+\gamma_{ref})^2}|s_{in}|^2 \end{cases}. \quad (2)$$

Apparently, the reflectance is smaller than one due to the loss of energy in the groove indicated by γ_0. Under the resonant condition, i.e., $\omega=\omega_0$, R gets the minimum value and the groove acts as a novel type of resonator in which only one SPP mode is excited. This case corresponds to the strongest localization of energy, as can be seen by the expression of $|a|^2$. In other words, we can determine the resonant frequency of the groove by comparing the localization of energy at different frequencies.

In order to deeply understand the localized modes of the groove, we have carried out FDTD simulation on the groove shown in Fig. 1. In the numerical simulations, the refractive index of silica was set as 1.45 and a Drude–Lorentz function was used to describe the dielectric constant of silver [15]. The thickness of the silver layer and the depth and width of the groove were made to be 750, 500, and 50 nm, respectively. The grid sizes in the x- and z-directions were chosen to be 2.5 and 5 nm and a perfectly matched layer boundary condition was employed in the numerical simulations.

The energy intensity distribution along the groove axis as a function of wavelength/frequency calculated by FDTD simulation is shown in Fig. 2. The positions of 0.0 and

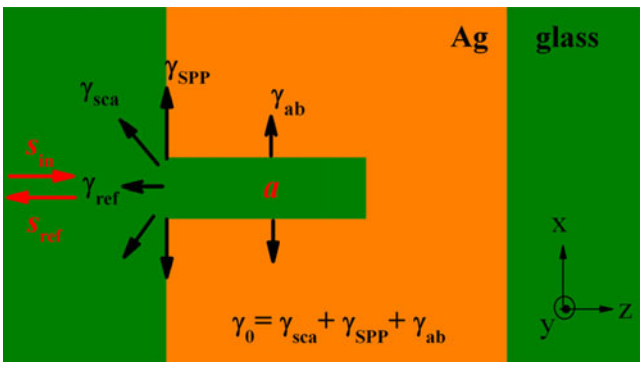

Fig. 1 Schematic of a *U*-shaped groove made in a thin silver layer (*orange color*) embedded in silica (*green color*). The *arrows* indicate the possible decay channels of the incident wave, including reflection, excitation of SPPs, and absorption

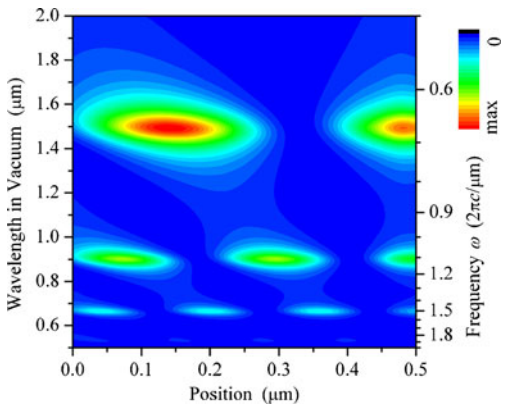

Fig. 2 Energy intensity distribution along the groove axis as a function of wavelength/frequency calculated by FDTD simulation. The positions of 0.0 and 0.5 μm correspond to the mouth and bottom of the groove

0.5 μm correspond to the mouth and bottom of the groove, respectively. It is noticed that strong localization of energy in the groove occurs at three wavelength regions. According to the analysis based on Eq. 2, the central wavelengths of these regions give the resonant wavelengths of the localized modes in the groove. They are determined to be 0.67, 0.90, and 1.52 μm (in vacuum), respectively. The corresponding frequencies are calculated to be 1.49 ($2\pi c/\mu m$), 1.11 ($2\pi c/\mu m$), and 0.66 ($2\pi c/\mu m$), where c is the speed of light in vacuum. In the following, we will focus on the groove mode located at 0.90 μm. Based on FDTD simulation, the total decay rate, which is defined as $\gamma=\gamma_0+\gamma_{ref}$, is derived to be $\omega_0/27$ while the decay rate of groove mode into the reflected wave γ_{ref} is found to be 0.7γ.

Two Side-Coupled Metallic Grooves

In the last section, we have analyzed theoretically by CMT and calculated numerically by FDTD simulation the localized modes of an isolated groove. Now we move on to the two identical grooves created on the two sides of the silver layer, as schematically shown in Fig. 3. If the two grooves are brought close, side coupling between them through evanescent wave tunneling is expected. As a result, a transmitted wave can be detected at the mouth of the right groove if an incident wave is launched normally on the left groove. In this case, the transmittance of the coupled grooves depends not only on the wavelength (or frequency) of the incident wave but also on the separation between the two grooves (denoted as d in Fig. 3). Here, the two grooves are designed to be side-coupled rather than butt-coupled (bottom to bottom) so that the coupling strength between them can be adjusted and especially enhanced by increasing the coupling length, which is indicated by l_c in Fig. 3. One of the advantages of this design is that the separation between the grooves is not necessary to be small which is difficult to realize in practice. Similar to directional couplers, we introduce two parameters, κ_{12} and κ_{21}, to characterize the cross couplings between the grooves.

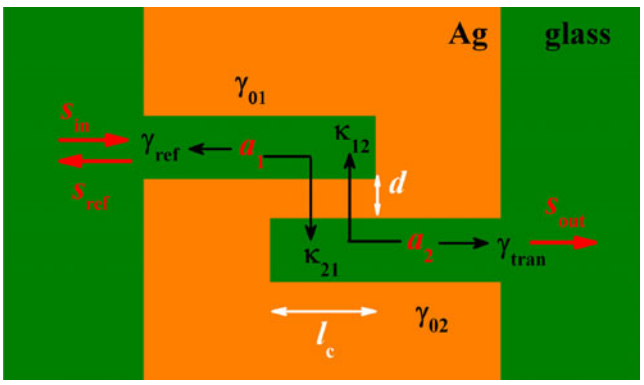

Fig. 3 Schematic of two side-coupled grooves created on the two sides of a silver layer. Here, d and l_c represent the coupling lengths between the grooves in the transverse and longitudinal directions, respectively

Assuming again that the incident wave is launched normally on the left groove, the amplitudes of the localized modes in the two grooves, denoted as a_1 and a_2, satisfy the following equation according to CMT

$$\begin{cases} \frac{da_1}{dt} = (j\omega_0 - \gamma_{ref} - \gamma_{01})a_1 + \kappa_{12}a_2 + \sqrt{2\gamma_{ref}}s_{in} \\ \frac{da_2}{dt} = (j\omega_0 - \gamma_{tran} - \gamma_{02})a_2 + \kappa_{21}a_1 \\ s_{ref} = -s_{in} + \sqrt{2\gamma_{ref}}a_1 \quad , \quad s_{out} = \sqrt{2\gamma_{tran}}a_2 \end{cases}, \tag{3}$$

where s_{out} is the normalized amplitude of the transmitted wave and $|s_{out}|^2$ represent the output power from the right groove, γ_{ref} (γ_{tran}) denotes the decay rate of a_1 (a_2) into the reflected (transmitted) waves, and γ_{01} (γ_{02}) denotes the total decay rate of a_1 (a_2) into other channels including scattering, excitation of SPPs, and absorption. Based on Eq. 3, the transmittance $T=|s_{out}/s_{in}|^2$, which reflects the transmission lineshape of the coupled grooves (i.e., $T(\omega)$), can be written as

$$T(\omega) = \left| \frac{2\sqrt{\gamma_{ref}\gamma_{tran}}\kappa_{21}}{\gamma_1\gamma_2 - \kappa_{12}\kappa_{21} - (\omega-\omega_0)^2 + j(\gamma_1+\gamma_2)(\omega-\omega_0)} \right|^2, \tag{4}$$

where $\gamma_1=\gamma_{ref}+\gamma_{01}$, $\gamma_2=\gamma_{tran}+\gamma_{02}$ can be considered as the total decay rates of a_1 and a_2, respectively. Since the two grooves are identical and we only discuss the coupling of the same localized modes, i.e., $\gamma_{ref}=\gamma_{tran}=\gamma_e$, $\gamma_{01}=\gamma_{02}=\gamma_0$, $\gamma_1=\gamma_2=\gamma$, and $\kappa_{12}=\kappa_{21}=j\kappa$, Eq. 4 can be rewritten as

$$\begin{aligned} T(\omega) &= \frac{4\gamma_e^2\kappa^2}{4\gamma^2\kappa^2 + \left[(\omega-\omega_0)^2 + \gamma^2 - \kappa^2\right]^2} \\ &= \frac{(\gamma_e/\gamma)^2}{1 + \frac{1}{4}\cdot\left[\frac{(\omega/\gamma-\omega_0/\gamma)^2}{(\kappa/\gamma)} + \frac{1}{(\kappa/\gamma)} - (\kappa/\gamma)\right]^2}. \end{aligned} \tag{5}$$

Based on Eq. 5, we can easily calculated the transmission lineshape of the two side-coupled grooves and the evolution of the lineshape with the structure parameter of κ/γ is shown in Fig. 4. In the calculations, (γ_e/γ) and (ω_0/γ) are chosen to be 0.7 and 27 which have been determined by FDTD simulation for the groove mode located at 0.90 μm. For strong cross-coupling cases in which $(\kappa/\gamma)>1$, two transmission peaks are found to appear at frequencies $\omega_{1,2}=\omega_0\pm(\kappa^2-g^2)^{1/2}$. The larger cross-coupling, the wider is the separation between the two peaks, as can be seen in Fig. 4. In Eq. 5, there are two kinds of power function, $(\omega-\omega_0)^2$ and $(\omega-\omega_0)^4$, in the denominator of T. It is interesting to note, however, that only $(\omega-\omega_0)^4$ survives

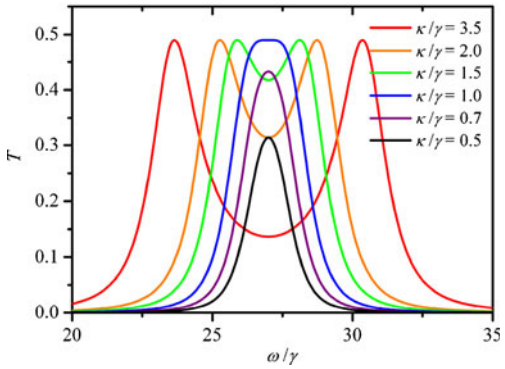

Fig. 4 Dependence of the transmittance lineshape on the cross coupling between two side-coupled grooves obtained by using Eq. 5. Here, γ_e/γ and ω_0/γ are chosen to be 0.7 and 27, respectively

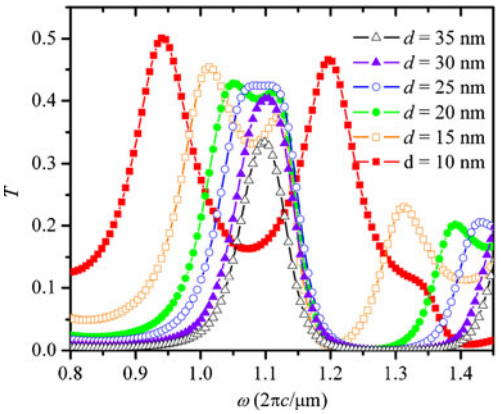

Fig. 5 Dependence of the transmittance lineshape on the separation between the two grooves obtained by FDTD simulations. The coupling length is fixed at l_c=250 nm

and the lineshape of T becomes flat-on-top when $(\kappa/\gamma)=1$. The lineshape like this is quite useful for optical filters. In the regime of weak cross-coupling, we have $(\kappa/\gamma)<1$ and only one peak is observed at ω_0 with a transmittance smaller than $(\gamma_e/\gamma)^2$. The smaller cross-coupling, the lower is the transmission peak. Therefore, Eq. 5 serves as an effective tool to analyze and understand the tunneling behavior of localized SPPs. It can be used to interpret the results shown in Fig. 2 of reference [8], though the coupling of two gratings rather than two grooves was investigated there. Furthermore, if we ignore the energy loss, i.e., we let $\gamma_e=\gamma$, Eq. 5 will become the formula (34) in reference [9] where strict derivations was employed for analyzing coupled gratings. It indicates that CMT can be utilized to describe the coupling of localized SPP modes.

In order to confirm the validity of the theoretical analysis based on CMT, we have performed FDTD simulations on the structure shown in Fig. 3. The structure parameters of the silver layer, the silica, and the grooves were chosen to be the same as those used for the isolated groove. The simulation parameters, including the grid size and the boundary condition, remained unchanged. For each frequency, a continuous wave was launched normally on the left groove at 100 nm in front of the groove mouth. The incident wave possesses a rectangular intensity distribution with a width of 100 nm. The power of the transmitted wave was measured by placing a 100-nm-wide monitor 20 nm away from the mouth of the right groove. The transmittance is defined as the ratio of the incident power to the transmitted power. We fixed the coupling length l_c=250 nm and adjusted the cross-coupling by changing the separation between the two grooves d. In this way, we obtain the evolution of the transmission spectrum with the change of the groove separation, as shown in Fig. 5. When d=35 nm, a single peak with a low transmittance of ~0.35 is observed due to weak cross coupling. As d is reduced to 30 nm, the lineshape of the transmission peak remains unchanged but a transmission enhancement is observed. A flat-on-top peak with a transmittance of ~0.40 is obtained when d is reduced to 25 nm. When d is further reduced to 20 nm, the cross coupling between the two grooves becomes strong and two peaks begin to appear in the lineshape. The separation between the two peaks becomes wider with decreasing d. For d=10 nm, we observe two widely separated peaks with a transmittance close to 0.50. Therefore, the theoretical prediction based on CMT is confirmed by numerical simulation based on the FDTD technique. However, the shapes of some transmission peaks look different, especially for the case of d=15 nm. This difference originates mainly from the influence of the adjacent groove modes, such as the modes located at 0.66 and 1.50 μm. When d is small, the coupling between neighboring groove modes cannot be neglected and it may affect the groove mode we studied, leading to the distortion of the lineshape which is not considered in the theoretical analysis. The asymmetric lineshape observed in Fig. 5 may be caused by the influences from the neighboring groove modes located at low and high frequencies.

Based on theoretical analysis and numerical simulation, we have known that the achievement of a flat-on-top transmission lineshape relies on the accurate control of the separation between the two grooves if the coupling length is fixed. Such a design can be implemented for other groove modes. Of course, the resonant frequency or wavelength of the groove mode can be modified by changing the structure parameters, mainly the depth of the grooves.

Conclusion

In summary, we have analyzed the localized modes of an isolated metallic groove and derived the transmission lineshape of two side-coupled metallic grooves in the framework of CMT. It is found that a single metallic groove acts a lossy optical resonator and the two side-coupled grooves function as an optical filter whose transmission lineshape

can be tailored by controlling the cross coupling between the two grooves. Particularly, optical filters with flat-on-top transmission lineshapes can be realized by making the cross coupling equal to the total decay rate of the groove mode. Theoretical analysis based on CMT is supported by numerical simulation based on the FDTD technique.

Acknowledgments The authors acknowledge the financial support from the National Natural Science Foundation of China (grant nos. 60778032, 10974060, and 51171066).

References

1. Lalanne P, Hugonin JP (2006) Interaction between optical nano-objects at metallo-dielectric. Nat Phys 2:551–556. doi:10.1038/nphys364
2. Pacific D, Lezec HJ, Atwater HA (2007) All-optical modulation by plasmonic excitation of CdSe quantum dots. Nat Photonics 1:402–406. doi:10.1038/nphoton.2007.95
3. Lopez-Tejeira F, Rodrigo SG, Martin-Moreno L, Garcia-Vidal FJ, Devaux E, Ebbesen TW, Krenn JR, Radko P, Bozhevolnyi SI, Gonzalez MU, Weeber JC, Dereux A (2007) Efficient unidirectional nanoslit couplers for surface plasmons. Nat Phys 3:324–328. doi:10.1038/nphys584
4. Bozhevolnyi SI, Volkov VS, Devaux E, Ebbesen TW (2005) Channel plasmon-polariton guiding by subwavelength metal grooves. Phys Rev Lett 95:046802. doi:10. 1103/PhysRevLett.95.046802
5. Ferry VE, Sweatlock LA, Pacifici D, Atwater HA (2008) Plasmonic nanostructure design for efficient light coupling into solar cells. Nano Lett 8:4391–4397. doi:10.1021/nl8022548
6. Min C, Veronis G (2009) Absorption switches in metal–dielectric–metal plasmonic waveguides. Opt Express 17:10757–10766. doi:10.1364/OE.17.010757
7. Lin XS, Huang XG (2008) Tooth-shaped plasmonic waveguide filters with nanometeric sizes. Opt Lett 33:2874–2876. doi:10.1364/OL.33.002874
8. Tan WC, Preist TW, Sambles RJ (2000) Resonant tunneling of light through thin metal films via strongly localized surface plasmons. Phys Rev B 16:11134–11138. doi:10.1103/PhysRevB.62.11134
9. Dykhne AM, Sarychev AK, Shalaev VM (2003) Resonant transmittance through metal films with fabricated and light-induced modulation. Phys Rev B 67:195402. doi:10.1103/PhysRevB.67.195402
10. Liu WC (2002) Optical tunneling effect of surface plasmon polaritons and localized surface plasmon resonance. Phys Rev B 65:155423. doi:10.1103/PhysRevB.65.155423
11. Lan YC, Chang CJ, Lee PH (2009) Resonant tunneling effects on cavity-embedded metal film caused by surface-plasmon excitation. Opt Lett 34:25–27. doi:10.1364/OL.34.000025
12. Wang LC, Deng L, Cui N, Niu YP, Gong SQ (2010) Extraordinary optical transmission through metal gratings with single and double grooved surfaces. Chin Phys B 19:017303. doi:10.1088/1674-1056/19/1/017303
13. Krishnan A, Thio T, Kim TJ, Lezec HJ, Ebbesen TW, Wolff PA, Pendry J, Martin-Moreno L, Garcia-Vidal FJ (2001) Evanescently coupled resonance in surface plasmon enhanced transmission. Opt Comm 200:1–7. doi:10.1016/S0030-4018(01)01558-9
14. Haus HA (1984) Wave and fields in optoelectronics. Prentice-Hall, New Jersey
15. Lee TW, Gray SK (2005) Subwavelength light bending by metal slit structures. Opt Express 13:9652–9659. doi:10.1364/OPEX.13.009652